

Original Articles

Changing patterns in farming–pastoral ecotones in China between 1990 and 2010

Li Shiji^{a,b}, Sun Zhigang^{a,b,*}, Tan Minghong^{b,c}, Guo Linlin^a, Zhang Xubo^a^a Key Laboratory of Ecosystem Network Observation and Modeling, Institute of Geographical Sciences and Natural Resources Research, Chinese Academy of Sciences, Beijing 100101, China^b College of Resources and Environment, University of Chinese Academy of Sciences, Beijing 100190, China^c Key Laboratory of Land Surface Pattern and Simulation, Institute of Geographical Sciences and Natural Resources Research, Chinese Academy of Sciences, Beijing 100101, China

ARTICLE INFO

Keywords:

Farming-pastoral ecotone (FPE)
Landscape pattern
Remote sensing
Land cover
Ecological protection policies

ABSTRACT

The farming-pastoral ecotone (FPE), defined as the mosaic of transition zone between traditional farming and pastoral regions, is sensitive to climate change and human disturbance. Extensive farming activities within and along FPEs have led to alarming environment degradation in China in the past several decades. Many ecological protection policies have been deployed to improve the structure and function of current FPEs. However, the changes in national FPE patterns as a result of farming activities and ecological protection policies have rarely been quantified using a robust dataset. Therefore, in this study we quantified two-decades of FPE change patterns in China using spatial autocorrelation and spatial clustering methods, along with land use data at 10 year intervals from 1990 to 2010. The results show that the derived FPEs in the north, middle, and south sections along the Hu's Line underwent remarkable spatio-temporal changes. The north and middle FPEs shifted from the southeast to northwest during the period of 1990–2000, mainly because of extensive farming activities. However, this trend slowed in the north FPE, and reversed in the middle FPE in the 2000s, mainly attributed to the deployment of ecological protection policies. As there are limited farming activities in mountainous terrains, the south FPE did not show notable changes compared with the north and middle FPEs. The FPE changes caused predominantly by extensive agricultural activities and ecological protection policies were then further quantified through transition matrix analyses between FPEs, farming areas (FA), and pastoral areas (PA). Our study suggests that new FPE maps derived from satellite remote sensing could provide a straightforward methodology to quantitatively evaluate the effect of agricultural activities and environmental policies on vulnerable FPE regions.

1. Introduction

Ecotones, defined as transition zones between landscape units (Metzger and Muller, 1996), are very sensitive to changes in the surrounding environment (He and Cui, 2015; Kamel, 2003; Reich et al., 2015). The farming-pastoral ecotone (FPE) is the mosaic transition zone between traditional farming and pastoral regions. The FPE can also be depicted as the region where farmlands invade into grassland boundaries (Liu et al., 2011). Significant attention has been placed on Chinese FPEs, where serious degradation has occurred owing to a rapid increase in farming and social-economic activities (Allen and Breshears, 1998; Lu and Jia, 2013; Xu et al., 2014). The desertification area in northern FPEs accounted for 36.5% of the total desertification in China in the late 1980s, and this ratio increased to 90% in 2000, at a rate of

approximately 2000 km² per year (Zhang and Li, 2000). In order to mitigate the environment degradation and achieve regional sustainable development, the Chinese government implemented a series of environmental protection and restoration policies, such as the Grain for Green (GFG) program, and directives for mitigating overgrazing in pasturing regions in the late 1990s (Delang and Yuan, 2015; Liu and Wu, 2010). These policies have changed land cover patterns; the implementation of the GFG program effectively decreased cultivated lands in or along FPEs after 2000 (Liu et al., 2014). However, in order to improve evaluations of policy effectiveness, the quantification of land use/land cover changes derived from satellite remote sensing images before and after policy implementations is a promising method. To date, however, such quantitative evaluations on environmental protection and restoration policies are rarely reported.

* Corresponding author at: Institute of Geographical Sciences and Natural Resources Research, Chinese Academy of Sciences, No.11A, Datun Road, Chaoyang District, Beijing 100101, China.

E-mail address: sun.zhigang@igsnrr.ac.cn (Z. Sun).

Several methods have been proposed to define FPEs based on the views of economic geography, agricultural climate, agricultural regionalization, and ecology (Fortin et al., 2000; Hufkens et al., 2009; Wu and Guo, 1994). Researchers that use climate indices to define FPE generally agree on the 400-mm isohyet to be the centerline, but have different opinions on the values of other indices to delineate the boundaries including the humidity index, inter-annual precipitation variability and threshold values of mean annual precipitation (Liu et al., 2011; Zhao et al., 2002). Wu and Guo (1994) proposed that the ratio of areas in cropland, grassland and forestland should be 1:0.5:1.5 to define the FPE in Northern China. However, the FPEs derived from these methods only delineate vague spatial boundaries with specific characteristics of climate, agriculture, economy, or ecology. FPE mapping using remote sensing-based land use/land cover with fine resolutions would provide a straightforward method to accurately quantify the geographic pattern of FPEs and their spatiotemporal changes.

In this study, we aim to map FPEs using land use data, investigate spatial and temporal changes in FPEs, and quantitatively evaluate the effects of protection policies on FPE changes in China during the past two decades.

2. Methodology

2.1. Data and preprocessing

Land use data with a spatial resolution of 1×1 km on a national scale were used to map FPEs in China in 1990, 2000, and 2010. The land use data product was accessed at the Data Center for Resources and Environmental Sciences, Chinese Academy of Sciences (RESDC, CAS; <http://www.resdc.cn>). The national land use dataset was developed at a spatial scale of 1:100,000 by visual interpretation and digitalization using Landsat TM/ ETM images and China-Brazil Earth Resources Satellite (CEBRS-1) images. Numerous field investigations have proved that the land use classification of this dataset had an accuracy of more than 90% (Liu et al., 2002; Liu et al., 2003, 2014), which can meet the requirement of mapping FPE accuracy on the 1:100,000-scale.

The area-percentage data model (APDM) has been extensively used to analyze the spatial-temporal features of land use change (Deng et al., 2006, 2010; Wang et al., 2010), and was utilized in this study to create a set of continuous variables for land use data. This data preprocessing was implemented using the Fishnet and Aggregate modules in ArcGIS (Liu et al., 2011; Tucker, 2000).

2.2. Mapping FPEs and drawing the study area

Spatial autocorrelation and spatial clustering methods could be combined to map FPEs in China (Xiao and Zhang, 2008) (Fig. 1). Spatial autocorrelation measures the degree to which a set of spatial features tend to be clustered (Legendre, 1993). To detect the heterogeneity of spatial features, in this study, the Local Indicators of Spatial Association (LISA) approach was used to evaluate the degree of spatial autocorrelation (local Moran's I) and the statistical significance of each point (Anselin, 2013).

The model equations are as follows:

$$I_i = \frac{(n-1)(X_i - \bar{X})}{\sum_{j=1, j \neq i}^n (X_j - \bar{X})^2} \sum_{j=1, j \neq i}^n \omega_{ij} (X_j - \bar{X}) \quad (1)$$

$$z(I_i) = \frac{I_i - E(I_i)}{\sqrt{\text{var}(I_i)}} \quad (2)$$

where I_i is the value of Local Moran's I in position i , n is the number of research objects, X_i is the observed value, X_j is the neighbor of X_i , \bar{X} is the mean of X_i , ω_{ij} is the spatial weight between research objects, and

$z(I_i)$ is the LISA z-test, which was tested at the 95 percent confidence level. In this study, FPEs were mapped through generating the area-percentage for cropland and grassland, producing maps of spatial clustering for cropland and grassland, and overlaying the clustering maps. Detailed procedures were shown in Fig. 1. Firstly, the APDM was used to generate continuous variables for cropland and grassland in 10×10 km grids. Secondly, the I_i values of cropland and grassland were calculated for all grids and then the significance test for I_i and the spatial clustering analysis were conducted using the GeoDa V1.6.7 tool (Anselin et al., 2006). Then the spatial clustering maps of cropland and grassland were outputted from the GeoDa tool based on the combination of I and p values. The clustering results of both cropland and grassland were divided into 5 types, respectively, including High-High (HH), Low-Low (LL), High-Low (HL), Low-High (LH), and Not Significant (NN). HH and LL, representing statistically significant clusters with high I values and low I values, indicate croplands (or grasslands) are highly clustered and dispersed in space, respectively. Both HL and LH, representing statistically significant spatial outlier data, indicate a high area-percentage value surrounded primarily by low area-percentage values (HL) and a low area-percentage value surrounded by high area-percentage values (LH), respectively. NN indicates no statistically significant in spatial cluster ($p > 0.05$). According to the criteria of spatial clustering classification (Table 1), thirdly, the paired cropland and grassland clustering maps were used to generate 4 landscape types, including Farming area (FA), Pastoral area (PA), Farming-Pastoral ecotone (FPE), and the Other area (OA). An artificial study area was defined to provide a reference space over which changes in FPEs could be quantified. Two steps were implemented to determine the study area (Fig. 2). Firstly, three FPE maps from 1990, 2000, and 2010 were overlaid to obtain a merged map. Then, the merged map was extended away from the boundary by a distance of 100 km using the ArcGIS buffer tool. This distance was determined by considering the maximum moving distance of FPE boundaries during the period of 1990–2010 was less than 100 km.

2.3. Transition matrix for analyses of land use changes

The transition matrix was used to quantify the conversions among investigated landscape types between two given dates. In this study, four landscape types were investigated, including FA, PA, FPE and OA.

3. Results

3.1. New Chinese FPE maps derived from land use data

Three new FPE maps from 1990, 2000, and 2010 across China were generated (Fig. 2). The FPEs cover 757 counties in 19 provinces, and accounts for about 37.7% and 59.4% of all the counties and provinces in China, respectively. Considering the vast differences in spatial patterns and geographical conditions, the Chinese FPEs were divided into three sections (north, middle, and south) for detailed investigations. Fig. 2 shows that the derived FPEs are located along the Hu's Line from the northeast to southwest of China. The Hu's Line, from the city of Heihe to Tengchong County, is a symbolic geographical line that divides China into two roughly equal parts, and was put forward by Huanyong Hu (Hu, 1990). This straight line was essential to understanding the spatial patterns of Chinese climate, terrain, population, and economy. Rather than rough spatial patterns of FPEs referring to economic development, agricultural climate, agricultural regionalization, and ecology, the satellite-based FPEs can be used to quantify accurate spatial patterns and areas. The cumulative average area of Chinese FPEs is $1.56 \times 10^6 \text{ km}^2$, accounting for about 1/5 of China's land area.

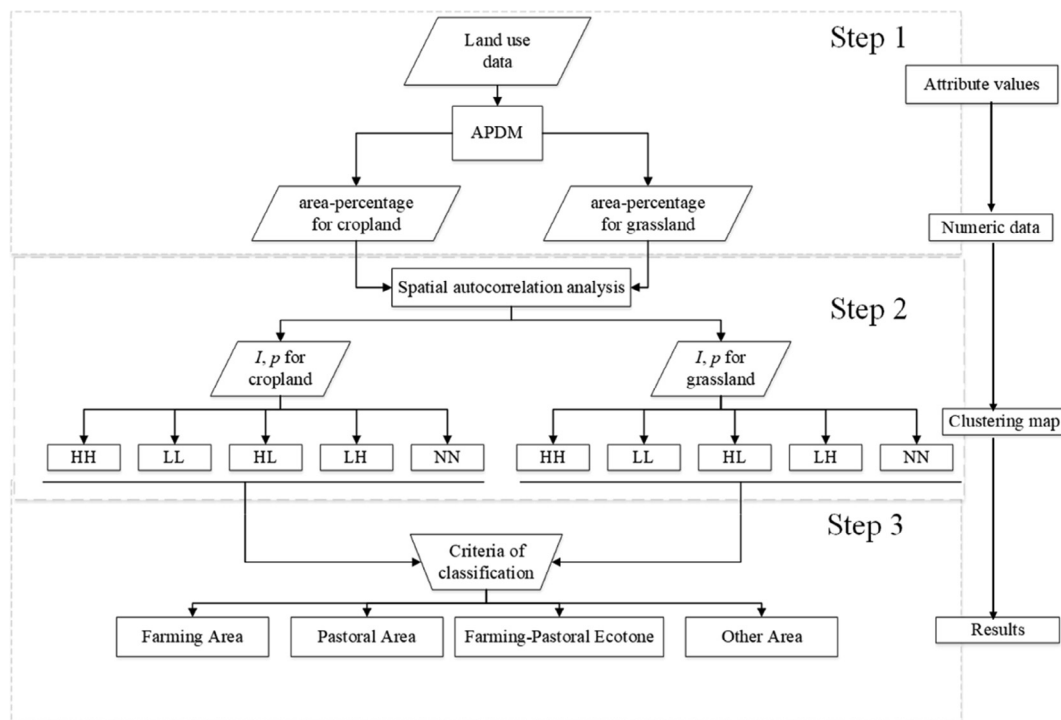


Fig. 1. Flowchart of FPE mapping in China.

Table 1

Criteria of classification based on spatial clustering (after Xiao and Zhang, 2008).

Farmland	Grassland	Type
Not Significant	Not Significant	FPE ^a
Not Significant	High-High	FPE
High-High	Not Significant	FPE
High-High	High-High	FPE
Not Significant	Low-Low	FA ^b
High-High	Low-Low	FA
Low-Low	Not Significant	PA ^c
Low-Low	High-High	PA
Low-Low	Low-Low	OA ^d

Notes: ^aFPE = Farming-Pastoral Ecotone^b FA = Farming Area^c PA = Pastoral Area^d OA = Other Area. To simplify the criteria of classification, we incorporated High-Low and Low-High types into Not Significant type for both cropland and grassland (Xiao and Zhang, 2008).

3.2. Changes in the spatial pattern of FPEs in China from 1990 to 2010

From Fig. 3, new Chinese FPE maps exhibit marked changes in time. The total FPE area in China decreased by 0.29% ($4.5 \times 10^3 \text{ km}^2$) from 1990 to 2000, and then increased 0.08% ($1.2 \times 10^3 \text{ km}^2$) from 2000 to 2010. Although changes in the north FPEs from 1990 to 2010 showed the same pattern to that of the total FPEs, the magnitudes of area change were quite different. The area of the north FPE sharply decreased by 6.47% ($1.9 \times 10^4 \text{ km}^2$) in the 1990s, and then slowly increased by 1.03% ($2.8 \times 10^3 \text{ km}^2$) from 2000 to 2010. The middle FPE area slightly increased by 0.29% ($2.6 \times 10^3 \text{ km}^2$) from 1990 to 2000, and then held relatively constant for the next decade. Differing from the north and middle FPEs, the south FPE areas sharply increased 3.18% ($1.1 \times 10^4 \text{ km}^2$) in the first decade, and then moderately decreased 0.76% ($2.8 \times 10^3 \text{ km}^2$) in the second decade. Fig. 4a and b capture how the FPE changes are quite different in geographical space among the north, middle, and south FPEs. The spatial changes of the FPEs were mainly distributed along the FPE boundaries, especially in north and south. Both farming (east) and pastoral (west) boundaries of the north

FPE moved notably westward from 1990–2000. The decreased FPEs clustered in the joint region of the Inner Mongolia Autonomous Region, Jilin, and Liaoning provinces. The increased FPEs mainly distributed along pastoral boundaries. After 2000, only sporadic changes occurred in FPEs along the conventional boundaries of the north FPE. Changes in the middle and south FPEs were different from the north FPE from 1990–2000. The FPE fluctuations were distributed intermittently along the farming and pastoral boundaries of the middle and south FPEs. However, after 2000 the changes were similar to the north FPE in that they were infrequent and irregularly distributed along the conventional boundaries of the middle and south FPEs.

3.3. Explanation of FPE changes using the transition matrices between FA, PA, and FPE

The change in FPEs could be further explained through the transition matrices between FA, PA, and FPE. As shown in Fig. 5 and Table 2, the westward-moving FPEs during 1990–2010 were mainly caused by the transition from FPE to FA along the eastern farming boundaries, and the transition from PA to FPE along the western pasture boundaries. Among the total land cover type transfers from FPEs during 1990–2000, the transferred area to FA was up to $8.15 \times 10^4 \text{ km}^2$, whereas the transferred area to PA was only $2.72 \times 10^4 \text{ km}^2$. During that same period, the opposite transfers (from FA and PA to FPEs) were comparable, with values of $5.42 \times 10^4 \text{ km}^2$ and $4.86 \times 10^4 \text{ km}^2$, respectively. However, the westward-moving trend notably eased after 2000, with the transferred area from FA to FPE ($2.62 \times 10^4 \text{ km}^2$) slightly less than FPE to FA ($2.68 \times 10^4 \text{ km}^2$), and transferred areas from PA to FPE ($1.66 \times 10^4 \text{ km}^2$) higher than FPE to PA ($1.45 \times 10^4 \text{ km}^2$), indicating grassland degradation was the main cause driving the FPE spatial shifts during 2000–2010.

3.3.1. North section

Same as the overall FPEs shift patterns, the westward-moving trend for the northern FPEs during 1990–2010 were mainly attributed to the transition from FPE to FA along farming boundaries, and the transition from PA to FPE along pasture boundaries. Among all land cover types

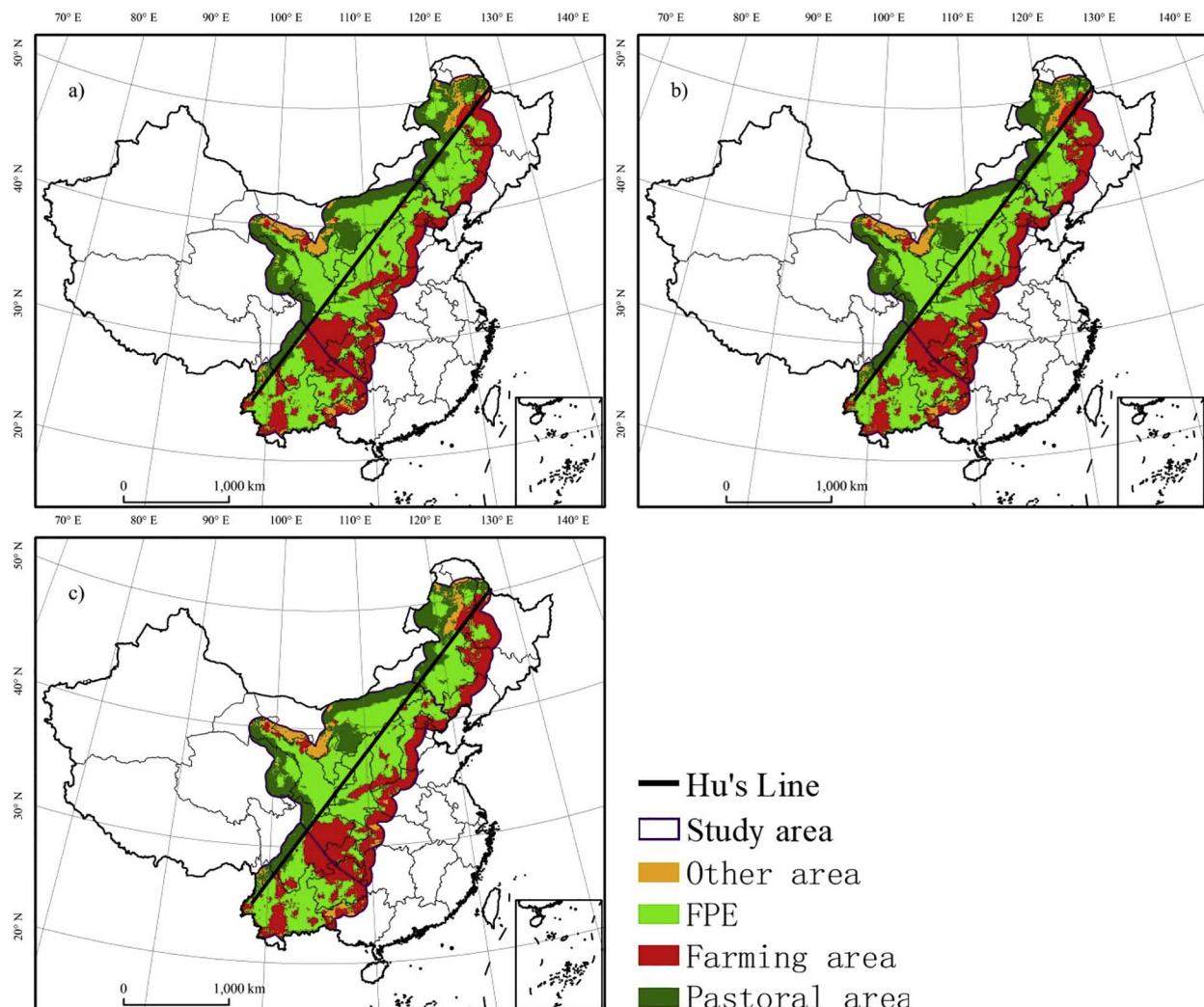


Fig. 2. Maps of the farming-pastoral ecotone in 1990 (a), 2000 (b), and 2010 (c) in China.

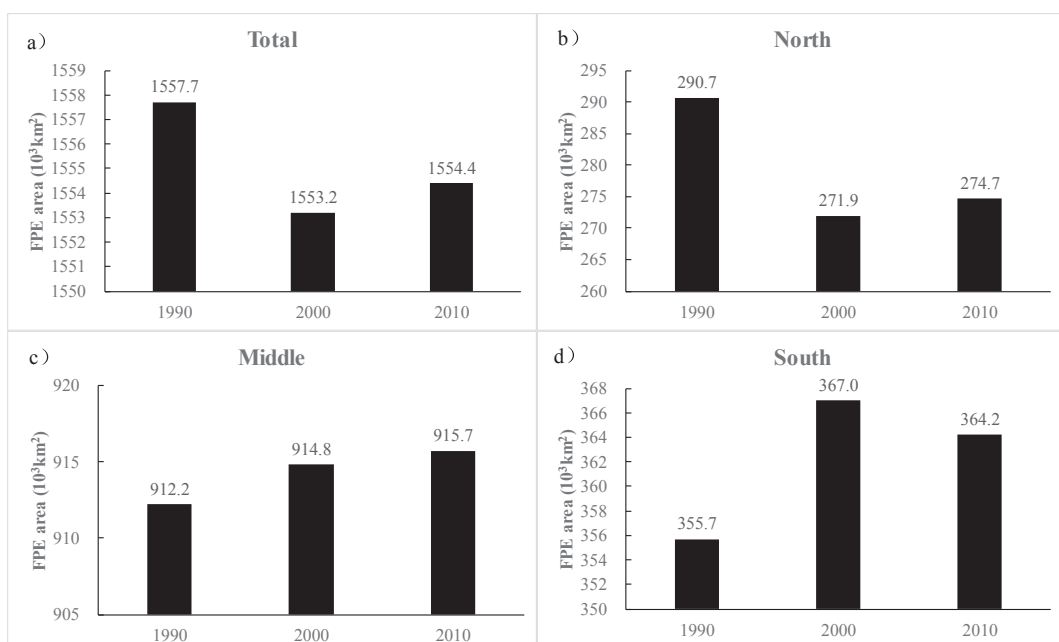


Fig. 3. Change in the area of total (a), north (b), middle (c), and south (d) FPEs in China.

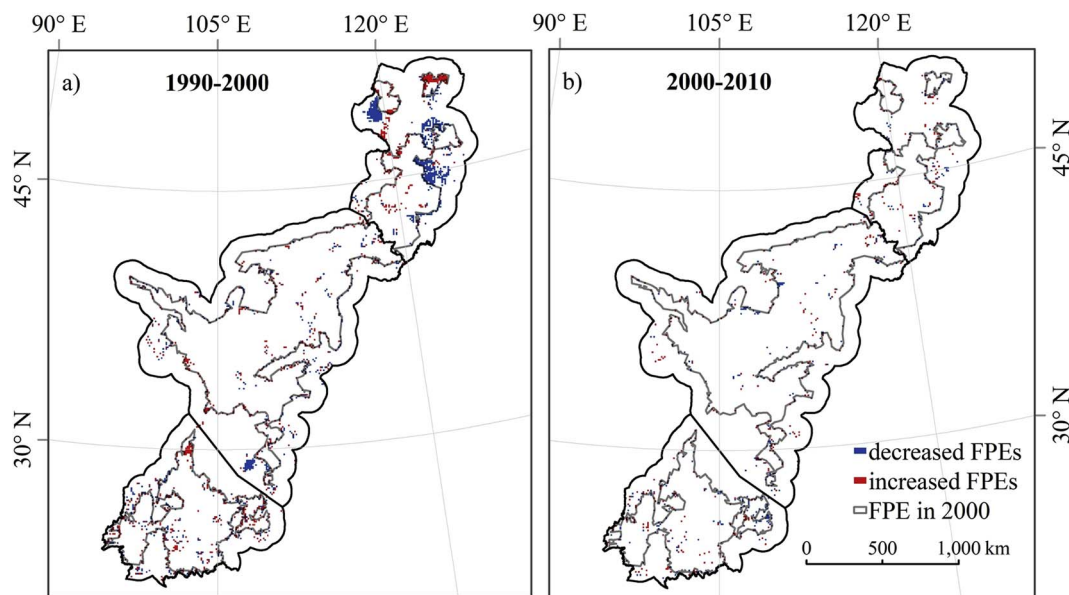


Fig. 4. Changes in the spatial patterns of FPEs in China for 1990 vs. 2000 (a), and 2000 vs. 2010 (b).

transferred to FPEs, the area from PA covered $2.70 \times 10^4 \text{ km}^2$ during 1990–2000, well above that of FA ($3.80 \times 10^3 \text{ km}^2$). In turn, area transferred from FPE to FA covered $3.83 \times 10^4 \text{ km}^2$, whereas the transferred area to PA was only $1.27 \times 10^4 \text{ km}^2$. However, the westward-moving trend markedly diminished after 2000, with higher transfer values from FA to FPE ($5.90 \times 10^3 \text{ km}^2$) than FPE to FA ($5.60 \times 10^3 \text{ km}^2$), as well as for PA to FPE ($6.80 \times 10^3 \text{ km}^2$) compared to FPE to PA ($4.30 \times 10^3 \text{ km}^2$). The results showed that the north section experienced noticeable farmland reclamation and grassland degradation during 1990–2000, whereas the reclamation had been effectively inhibited after 2000.

3.3.2. Middle section

The moving trends of the middle FPE regions showed notable differences to the total and north FPEs during 2000–2010. Among all land cover types transferred into the FPE during 1990–2000, area from FA and PA covered $2.12 \times 10^4 \text{ km}^2$ and $1.60 \times 10^4 \text{ km}^2$, respectively. In turn, area transferred from FPE to FA covered $2.58 \times 10^4 \text{ km}^2$, whereas

the transferred area to PA was only $8.80 \times 10^3 \text{ km}^2$. However, the moving direction thoroughly reversed after 2000, with the area values transferred from FA to FPE ($1.08 \times 10^4 \text{ km}^2$) being higher than FPE to FA ($9.60 \times 10^3 \text{ km}^2$), and the transferred area from PA to FPE ($6.90 \times 10^3 \text{ km}^2$) was less than FPE to PA ($7.30 \times 10^3 \text{ km}^2$). The results illustrated that both the reclamation and degradation were effectively improved for the middle section during 2000–2010.

3.3.3. South section

Different from the other sections, the FPE variation in the south section was limited by mountainous terrain. Table 2 shows that the mutual transformation of FA and FPE predominated the transition of FPE over the last two decades. The continued decline of cultivated areas contributed to the transferring from FA to FPE during 1990–2010. Taking the Lushan county as an example, which is located at the western edge of the Sichuan Basin, the cropland has dropped from 7600 ha in 1990 to 4242 ha in 2010, a statistical decrease of 44.18%.

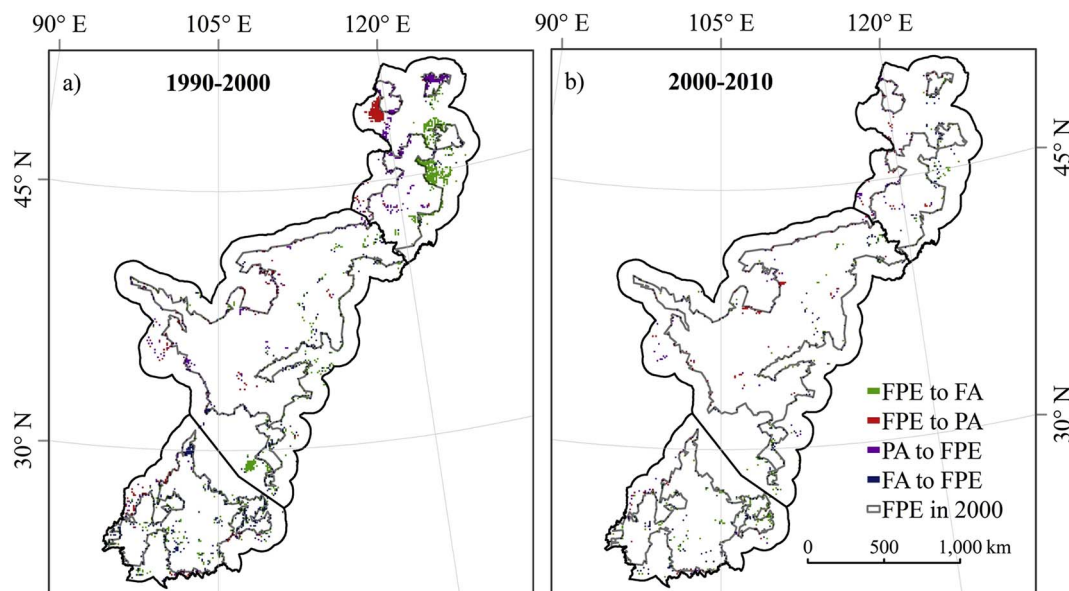


Fig. 5. Interconversion between FA, PA and FPE in study area for 1990 vs. 2000 (a), and 2000 vs. 2010 (b).

Table 2
Transitions between FA, PA and FPE during 1990–2010 ($\times 10^4 \text{ km}^2$).

	Total	North	Middle	South
FA → FPE ^a	1990–2010	5.63	0.50	2.30
	1990–2000	5.42	0.38	2.12
	2000–2010	2.62	0.59	1.08
PA → FPE ^b	1990–2010	5.16	2.83	1.71
	1990–2000	4.86	2.70	1.60
	2000–2010	1.66	0.68	0.69
OA → FPE ^c	1990–2010	0.18	0.10	0.01
	1990–2000	0.20	0.14	0.01
	2000–2010	0.01	0	0.01
FPE → FA ^d	1990–2010	8.38	3.86	2.63
	1990–2000	8.15	3.83	2.58
	2000–2010	2.68	0.56	0.96
FPE → PA ^e	1990–2010	2.85	1.17	1.03
	1990–2000	2.72	1.27	0.88
	2000–2010	1.45	0.43	0.73
FPE → OA ^f	1990–2010	0.07	0	0.01
	1990–2000	0.06	0	0.01
	2000–2010	0.04	0	0.04

^{a,b,c} FA→FPE, PA→FPE, OA→FPE: represent that among all the other types transferred into FPE, the area FA/PA/OA covered; ^{d,e,f}FPE→FA, FPE→PA, FPE→OA: represent the area transferred from FPE to FA/PA/OA.

4. Discussions

4.1. Evaluation on new FPE map derived from satellite land use data

The proposed FPE map differed from previous FPE maps derived from climatic, agricultural, economic, or ecologic indices. For example, the climate-based FPE map in northern China approximately parallels with our proposed FPE map (Liu et al., 2011; Xu et al., 2014; Yang et al., 2012) but differs in tilt angle and width (Fig. 6). The climate-based FPEs tend to shift northwest in southwestern China. However, alpine meadow and alpine grasslands dominate in northwest-shifted FPEs where farmland is sporadically distributed (Zhang et al., 2009). Rather than climate, the actual geographic distribution of FPE could be

reshaped by anthropogenic activities such as overgrazing and reclamation (Shi et al., 2017). The FPE map based on county-level GDPs (Gross Domestic Product) of farming and animal husbandry was artificially constrained with administrative boundaries. Therefore, the economy-based FPE could not delineate the actual FPE map. Comparing to climate- and economy-based FPE maps, therefore, the proposed new FPE map based on satellite remote sensing could be more objective and more accurate to quantify the FPE patterns and their changes in time and space.

4.2. The effects of climatic and anthropogenic factors on FPE changes

Under the background of global warming, China has experienced a remarkable increase in mean air temperature, especially in northern China, at a rate of 0.8 °C per decade in the last 50 years (Dong et al., 2009; Yang et al., 2011). Increased thermal conditions increased the northern and western limits of crop planting potential (Liu et al., 2013; Peters et al., 2014; Yang et al., 2015). Specifically, extensive agricultural developments within or along FPE boundaries caused FPEs to move northward and westward, resulting in grassland degradation and serious desertification prior to 2000. The central and local governments implemented a series of environmental protection and restoration policies to slow, and even reverse, the northward and westward FPE trends of the late 1990s (Delang and Yuan, 2015; Liu and Wu, 2010). Therefore, the spatial and temporal changes in FPEs were the combined result of climatic (climate warming) and anthropogenic factors (extensive farming and government protection policies) (Fig. 7). The north and middle FPEs had obvious northwestward-moving trends during 1990–2000. For the north section, the change in the north FPE was mainly attributed to the over-reclamation of croplands. The FA area increased by $3.87 \times 10^4 \text{ km}^2$ (20.62%) along the farming boundary, and the PA area decreased by $1.28 \times 10^4 \text{ km}^2$ (5.37%) along the pasture boundary during 1990–2000 (Table 3). This resulted in a net decrease in the north FPE area by 10.25%, and a northwestward contraction of the north FPE. For the middle section, the change in the middle FPE was mainly attributed to the degradation of grasslands. The FA area increased by $3.70 \times 10^3 \text{ km}^2$ (0.76%) and the PA area decreased by $1.02 \times 10^4 \text{ km}^2$ (2.68%) during 1990–2000, resulting in a

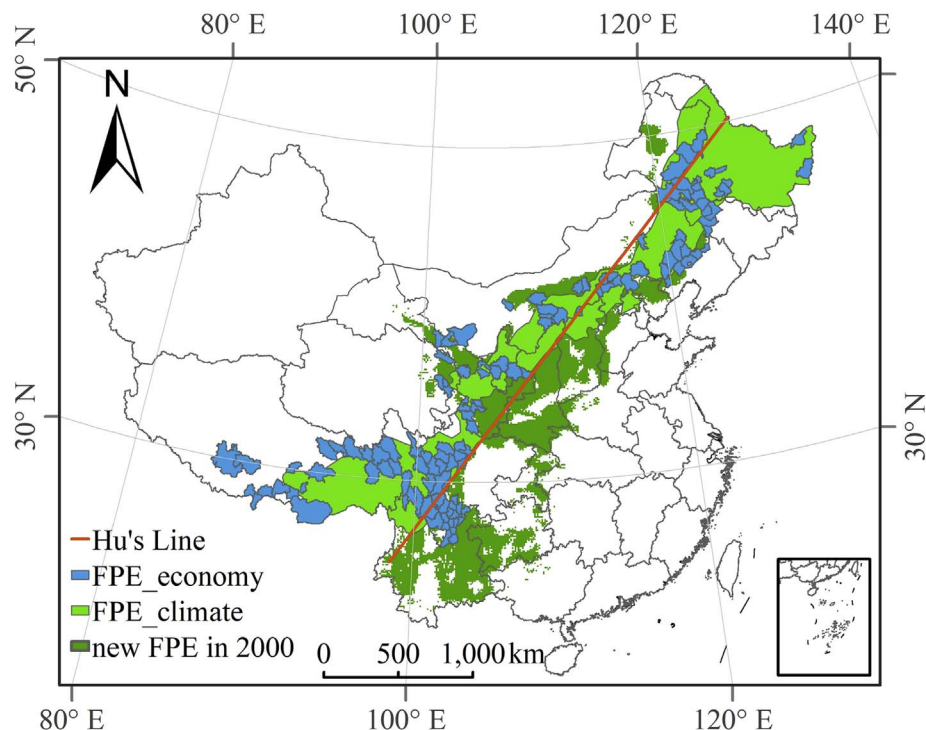
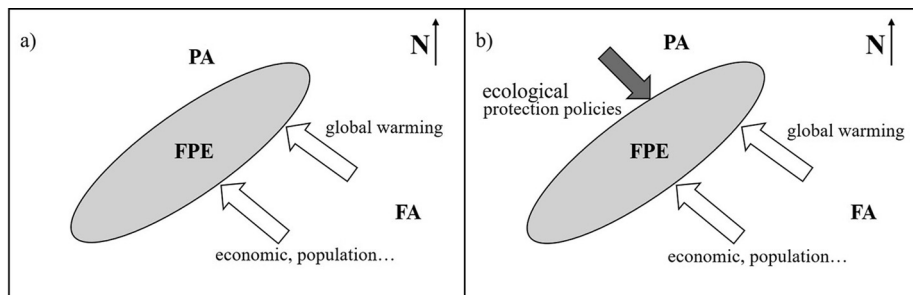


Fig. 6. Comparisons of published FPE maps based on climate, economy, and remote sensing. The FPE_climate refers to the map based on climatic factors, which was vectorized after Zhang et al. (2009); the FPE_economy refers to the map based on economic factors, which was delineated based on the list of FPE counties offered by the National Bureau of Statistics of China (Zhang, 2011); and the new FPE refers to the map based on remote sensing approach, which was proposed in this study.

**Table 3**

Changes in the ratios of FA and PA areas to referenced areas during 1990–2000 and 2000–2010.

	FA		PA	
	1990–2000	2000–2010	1990–2000	2000–2010
Total	2.90%	0.23%	−3.06%	−0.73%
North	20.62%	−0.09%	−5.37%	−2.16%
Middle	0.76%	−0.06%	−2.68%	−0.14%
South	−4.41%	0.99%	1.14%	−0.11%

modest net increase in the middle FPE by 0.29%, and a northwestward expansion of the middle FPE. However, the northwestward migration of the north and middle FPEs was slowed and even reversed after 2000, mainly owing to the deployment of protection policies. For the north section, the FA area reversely decreased by 200 km^2 (0.09%) and the PA area slowly decreased by $4.40 \times 10^3 \text{ km}^2$ (2.16%) during 2000–2010. This resulted in a slow northwestward expansion of the north FPE. The Tongyu County located in the west of Jilin Province was taken as an example for detailed investigation, where two distinct conversion patterns occurred, namely, FPE → FA during 1990–2000 and FA → FPE after 2000 (Fig. 8). The farmland in this county rapidly expanded during 1990–2000, resulting in the sharp decrease in the ratio of FPE area to total area from 97.59% to 36.14%. Owing to the GFG policy initiated in late 1990s, about $2.2 \times 10^3 \text{ km}^2$ (more than 10.00%) and about 117.20 km^2 (about 5.86%) of sloping farmlands (slope > 15°) were returned to grassland and forestry, respectively, after 2000. This resulted in an increase in FPE area by 6.02%. Although the GFG policy worked by limiting the expansion of cultivated land along the farming boundary in the north FPE, the grasslands along the pastoral boundary still continuously degraded. This suggests that further policies are required to relieve grazing intensity and protect grasslands in the north section. In the middle section, the FA and PA areas decreased respectively by 300 km^2 (0.06%) and 500 km^2 (0.14%) during 2000–2010,

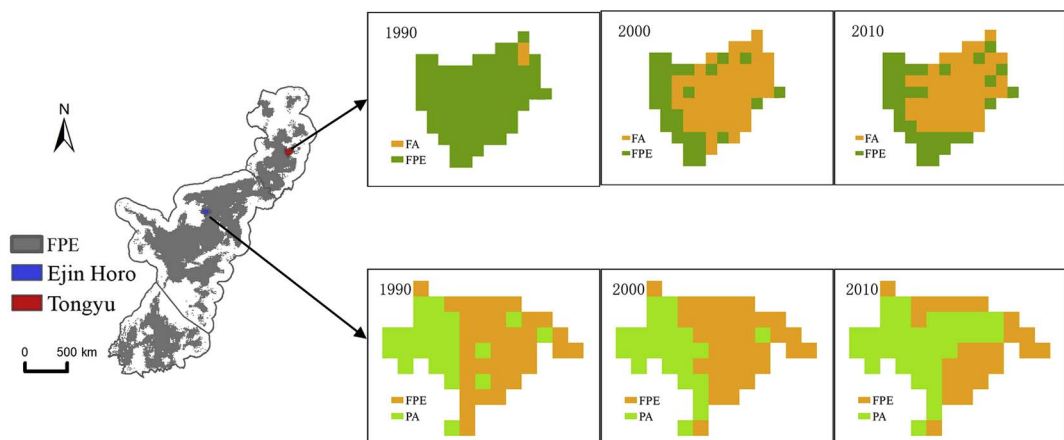
indicating that both farmland reclamation and grassland degradation was effectively under control. The Ejin Horo Banner (equivalent to a county in Inner Mongolia) located on the border between FPE and PA was taken as an example to demonstrate where significant FPEs were converted to PA, and grasslands markedly improved after 2000 (Fig. 8). Owing to the implementation of a range of policies, including the GFG program and policies of mitigating overgrazing in pasturing regions, the ratio of grassland area to total area of the Ejin Horo Banner increased from 40.64% prior to 2000 to 70.72% after 2000 (Chen et al., 2016), and the FPE area in this banner decreased by 1.67% over two decades.

4.3. Limitations and perspective

Although satellite remote sensing data was used to generate new Chinese FPE maps and further investigations were conducted to understand the spatiotemporal changes in FPEs, several limitations should be addressed in future studies. Firstly, the effect of spatial resolution of remote sensing data should be investigated. Scale effect was a crucial scientific challenge in landscape ecology studies (Bogucki and Turner, 1987; Li, 2015). The FPE areas commonly tend to increase with the scale of the remote sensing data used, and the FPE boundaries tend to be coarser. In this study we chose a 10 km grid size for the analysis scale, in order to keep consistent with previous studies (Xiao and Zhang, 2008). In future studies, this scale could be determined depending on the spatial resolution of remote sensing data available and the spatial accuracy of new FPE maps. Secondly, we evaluated the effects of ecological protective projects on FPEs only through comparing the spatiotemporal changes in FPE maps between two historical periods. Indicators regarding ecological qualities in FPEs could be included to further evaluate the effects of implemented policies on FPEs in future studies.

5. Conclusions

By integrating spatial autocorrelation and spatial clustering

**Fig. 8.** Changes in land cover types in case study areas during 1990–2010.

methods with remote sensing-based land use data, this study mapped the spatial and temporal distribution of FPEs in China, facilitating the examination of the effectiveness of the country's protection policies by a comparative analysis method. The following conclusions were reached. The FPE pattern changes showed remarkable regional differences. The Chinese FPEs defined in this study accounted for $1.56 \times 10^6 \text{ km}^2$ in average, about 1/5 of China's total land area. Different from the middle and south FPEs, the north FPE showed the most dramatic changes in area, with a sharp decrease by 6.47% ($1.9 \times 10^4 \text{ km}^2$) in the 1990s. It experienced marked farmland reclamation with significant westward migrations, especially at the juncture of the three provinces, Inner Mongolia Autonomous Region, Jilin, and Liaoning provinces. The transition matrices between FA, PA and FPE were employed. The results showed that both the north and middle FPEs experienced westward migration trends during 1990–2000, with the increase of FA (20.62% and 0.76%, respectively) and decrease of PA (5.37% and 2.68%, respectively). The shifting trends have been eased in the north FPEs, and were thoroughly reversed in the middle FPEs during 2000–2010 (Tab. 2). These results further verified that the implementation of the protection policies has changed the land use/land cover types significantly in the study area, especially the farmland and grassland. Finally, case studies were adopted for detailed investigation, and the results inferred that the protection policies have effectively prevented shifting trends for the north and middle FPEs. Moreover, policies for grassland protection should be further strengthened in pastoral (west) boundaries in the north FPE. For a more comprehensive and deeper evaluations of the effects of policy implementation for FPEs, ecological quality indicators could be included in future studies.

Acknowledgments

This research was supported by the National Key Research and Development Program of China (2017YFC0503805), the 100 Talents Program of the Chinese Academy of Sciences, National Natural Science Foundation of China (31570472), and the Science and Technology Service Network Initiative of the Chinese Academy of Sciences (KJF-EW-STS-054).

References

- Allen, C.D., Breshears, D.D., 1998. Drought-induced shift of a forest–woodland ecotone: rapid landscape response to climate variation. *Proc. Natl. Acad. Sci.* 95 (25), 14839–14842.
- Anselin, L., 2013. Spatial econometrics: methods and models, 4. Springer Science & Business Media.
- Anselin, L., Syabri, I., Kho, Y., 2006. GeoDa: an introduction to spatial data analysis. *Geogr. Anal.* 38 (1), 5–22.
- Bogucki, D.J., Turner, M.G., 1987. Landscape heterogeneity and disturbance. Springer.
- Chen, X.J., Yang, J., Hu, G.J., Chen, Y.Q., Hou, H., 2016. Effects of conversion of degraded farm land into forest (grass) on land use/ cover change in Ejin Horo Banner. *J. Inner Mongolia Univ.* 47 (5), 542–548 (in Chinese).
- Delang, C.O., Yuan, Z., 2015. China's Grain for Green Program. Springer.
- Deng, X., Huang, J., Rozelle, S., Uchida, E., 2006. Cultivated land conversion and potential agricultural productivity in China. *Land Use Policy* 23 (4), 372–384.
- Deng, X., Jiang, Q.O., Su, H., Wu, F., 2010. Trace forest conversions in Northeast China with a 1-km area percentage data model. *J. Appl. Remote Sens.* 4 (1) 041893–041893-13.
- Dong, J., Liu, J., Tao, F., Xu, X., Wang, J., 2009. Spatio-temporal changes in annual accumulated temperature in China and the effects on cropping systems, 1980s to 2000. *Clim. Res.* 40 (1), 37–48.
- Fortin, M., Olson, R., Ferson, S., Iverson, L., Hunsaker, C., Edwards, G., Levine, D., Butera, K., Klemas, V., 2000. Issues related to the detection of boundaries. *Landscape Ecol.* 15 (5), 453–466.
- He, Q., Cui, B., 2015. Multiple mechanisms sustain a plant-animal facilitation on a coastal ecotone. *Sci. Rep.* 5, 8612.
- Hu, H., 1990. The distribution, regionalization and prospect of China's population. *Acta Geographica Sinica* 2, 139–145 (in Chinese with English abstract).
- Hufkens, K., Scheunders, P., Ceulemans, R., 2009. Ecotones in vegetation ecology: methodologies and definitions revisited. *Ecol. Res.* 24 (5), 977–986.
- Kamel, M., 2003. Ecotone classification according to its origin. *Pak. J. Biol. Sci.* 6 (17), 1553–1563.
- Legendre, P., 1993. Spatial autocorrelation: trouble or new paradigm? *Ecology* 74 (6), 1659–1673.
- Li, W.H., 2015. Contemporary Ecology Research in China. Springer.
- Liu, C., Wu, B., 2010. Grain for Green Programme in China: policy making and implementation. *Policy Brief Ser.*(60).
- Liu, J., Liu, M., Deng, X., Zhuang, D., Zhang, Z., Luo, D., 2002. The land use and land cover change database and its relative studies in China. *J. Geog. Sci.* 12 (3), 275–282.
- Liu, J., Liu, M., Zhuang, D., Zhang, Z., Deng, X., 2003. Study on spatial pattern of land-use change in China during 1995–2000. *Sci. China Earth Sci.* 46 (4), 373–384 (in Chinese with English abstract).
- Liu, J.H., Gao, J.X., Lv, S.H., Han, Y.W., Nie, Y.H., 2011. Shifting farming-pastoral ecotone in China under climate and land use changes. *J. Arid Environ.* 75 (3), 298–308.
- Liu, J.Y., Kuang, W.H., Zhang, Z.X., Xu, X.L., Qin, Y.W., Ning, J., Zhou, W.C., Zhang, S.W., Li, R.D., Yan, C.Z., 2014. Spatiotemporal characteristics, patterns, and causes of land-use changes in China since the late 1980s. *J. Geog. Sci.* 24 (2), 195–210.
- Liu, Z.J., Yang, X.G., Chen, F., Wang, E.I., 2013. The effects of past climate change on the northern limits of maize planting in Northeast China. *Clim. Change* 117 (4), 891–902.
- Lu, W., Jia, G.S., 2013. Fluctuation of farming-pastoral ecotone in association with changing East Asia monsoon climate. *Clim. Change* 119 (3–4), 747–760.
- Metzger, J.P., Muller, E., 1996. Characterizing the complexity of landscape boundaries by remote sensing. *Landscape Ecol.* 11 (2), 65–77.
- Peters, K., Breitsameter, L., Gerowitt, B., 2014. Impact of climate change on weeds in agriculture: a review. *Agron. Sustain. Dev.* 34 (4), 707–721.
- Reich, P.B., Sendall, K.M., Rice, K., Rich, R.L., Stefanski, A., Hobbie, S.E., Montgomery, R.A., 2015. Geographic range predicts photosynthetic and growth response to warming in co-occurring tree species. *Nat. Clim. Change* 5 (2), 148–152.
- Shi, W., Liu, Y., Shi, X., 2017. Development of quantitative methods for detecting climate contributions to boundary shifts in farming-pastoral ecotone of northern China. *J. Geogr. Sci.* 27 (9), 1059–1071.
- Tucker, C., 2000. Using ArcToolbox: GIS by ESRI. Esri Press.
- Wang, S.Y., Liu, J.S., Ma, T.B., 2010. Dynamics and changes in spatial patterns of land use in Yellow River Basin, China. *Land Use Policy* 27 (2), 313–323.
- Wu, C., Guo, H., 1994. Land use in China (in Chinese). Chinese Science & Technology Press, Beijing.
- Xiao, L.X., Zhang, Z.X., 2008. Processes on the boundary definition of agro-pastoral zone in China. *Progr. Geogr.* 27 (2), 104–111 (in Chinese with English abstract).
- Xu, D.Y., Li, C.L., Song, X., Ren, H.Y., 2014. The dynamics of desertification in the farming-pastoral region of North China over the past 10 years and their relationship to climate change and human activity. *Catena* 123, 11–22.
- Yang, X.C., Xu, B., Jin, Y.X., Li, J.Y., Zhu, X.H., 2012. On grass yield remote sensing estimation models of China's Northern Farming-Pastoral Ecotone. In: Lee, G. (Ed.), *Advances in Computational Environment Science. Advances in Intelligent and Soft Computing*. Springer-Verlag, Berlin, Berlin, pp. 281–291.
- Yang, X.G., Chen, F., Lin, X.M., Liu, Z.J., Zhang, H.L., Zhao, J., Li, K.N., Ye, Q., Li, Y., Lv, S., Yang, P., Wu, W.b., Li, Z.g., Lal, R., Tang, H.j., 2015. Potential benefits of climate change for crop productivity in China. *Agric. For. Meteorol.* 208, 76–84.
- Yang, X.G., Liu, Z.J., Chen, F., 2011. The possible effect of climate warming on northern limits of cropping system and crop yield in China. *Agric. Sci. China* 10 (4), 585–594.
- Zhang, D.F., Li, F.Q., 2000. Mechanism of formation of fragile eco-environment of agro-pastoral zigzag zone in northern China. *Rural Eco-Environ.* 16 (4), 58–60 (in Chinese with English abstract).
- Zhao, H., Zhao, X., Zhang, T., Zhou, R., 2002. Boundary line on agro-pasture zigzag zone in north China and its problems on eco-environment. *Adv. Earth Sci.* 17 (5), 739–747.
- Zhang, J., Wei, J., Chen, Q., 2009. Mapping the farming-pastoral ecotones in China. *J. Mountain Sci.* 6 (1), 78–87.
- Zhang, S.Y., 2011. China county statistical yearbook 2011 (in Chinese). China Statistics Press, Beijing.